DOI:
10.1109/IROS.2016.7759333

Document Version
Early version, also known as pre-print

New Kinematic Multi-Section Model for Catheter Contact Force Estimation and Steering

Junghwan Back, Lukas Lindenroth, Rashed Karim, Kaspar Althoefer, Kawal Rhode, and Hongbin Liu*

Abstract*— Contact force play a significant role on success of the cardiac ablation. However it is still challenging to estimate contact force when catheter is under large bending and multiple contacts. This paper develops a new multi-section static model of tendon driven catheters for both real-time intrinsic force sensing and interaction control. The model allows the external force to be applied at arbitrary location on the catheter and can also cope with multiple contacts. In this study, we validated the model using a robotic platform, which steers a catheter consisting of 4 tendons with tension feedback. The experimental results show that the model can accurately predict the catheter shape with the effect of internal friction and large deflection. The position difference between measured and estimated was 2.5mm. Based on the catheter model, we developed an algorithm to estimate the contact force based on the catheter tip tracking and tension feedback. The validation results show that 3-dimensional contact forces can be estimated accurately using the proposed method. The magnitude of contact force error was 0.0117N with 400Hz update rate.

I. INTRODUCTION

Catheter ablation is an increasingly used minimally invasive procedure to treat arrhythmias when medications are unable to restore the normal heart rhythm. During the procedure, a steerable catheter is inserted into the heart to ablate targeted areas commonly using radio frequency energy (RF) to block abnormal electrical signals. Recent *in vivo* and *ex vivo* ablation studies demonstrated that the catheter contact force play a significant role on success of the procedure: the contact force is highly correlated with the size and depth of the ablation lesion, as well as the risk of complications [1-2]. Insufficient contact force tends to generate ineffective lesions; excessive contact force is associated with high incidences of popping and perforation.

However it is challenging to estimate the contact force during catheter ablation. The cardiologists have very limited haptic feedback during manual procedures since the contact force can be only partially transmitted to their fingers though the long and flexible body of the catheter. Tele-operation of the ablation catheters reduces the radiation exposure to the cardiologist but also eliminates their sense of touch. The importance of knowing the contact force during ablation has motivated the developments of catheter force sensor. For instance, the Thermocool® SMARTTOUCHTM catheter from Biosense Webster and the Sensei® catheter system provide both magnitude and direction of contact forces in their 3D visualized environments Carto® and NIOBE® respectively. However, it is both technically challenging and high cost to sensorize the catheters under the minimally invasive constraint.

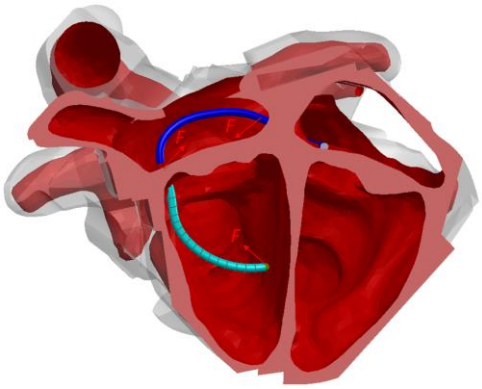

Fig.1.The concept of using multi-section catheter model to estimate the contact forces and to control the catheter.

The inherent flexibility of catheter makes it possible to use its flexible body as the sensor to estimate contact forces. Various efforts have been made in line with this concept. This intrinsic force sensing for continuum-like robots was introduced in [3] based on static modelling the robot assuming multiple constant curvature segments. Intrinsic force sensing for a thin continuum robot using a probabilistic approach is proposed in [6]. An extended Kalman filter was implemented to estimate the interaction forces given the measurements of robot pose. The feasibility has been demonstrated through simulation. Khoshnam et al [7] modeled the catheter as rigid-links manipulator to relax the constant curvature assumption. Based on the set up an index to estimate contact force levels based on the experimentally observed the curvature changes with respect to the applied forces. Our recent work shows that contact force at the catheter tip can be accurately estimated using a discretized Cosserat rod model with a given the catheter shape [8].

Kinematic modelling of catheter is the key factor to determine the accuracy of force estimation. However existing analytical kinematics models are mostly based on the assumption of constant curvature [3-5]. Previous research [9] and experimental observation have shown that the constant curvature assumption is invalid with the existence of internal friction and external forces, both of which are highly

Junghwan Back, Lukas Lindenroth, Kaspar Althoefer and Hongbin Liu are with Department of Informatics, King's College London, UK, WC2R 2LS.

Rashed Karim, and Kawal Rhode are with Department Imaging and Biomedical Engineering, King's College London, UK, SE1 7EH.

*indicates the correspond author, email{ hongbin.liu@kcl.ac.uk}

Preprint submitted to 2016 IEEE/RSJ International Conference on Intelligent Robots and Systems. Received March 1, 2016.

associated with catheter ablation. The empirical rigid-links model proposed in [7] can cope with variable curvature, but the model parameters need to the experimentally tuned for different catheters and bending configurations. Considerable research has been done on the modelling of large deflection of flexible body, such as Cosserat Rod model [10] and the co-rotational beam model [11]. These models can cope with the variable curvature under large deflection. However the prediction from applied force to shape deflection needs numerical integration. Thus, these model is computational expensive and not suitable for real-time application. Moreover, the existing models for catheters all assume that the contact occurs at the distal tip. However since the catheter is operated within the confined spaces in the heart, there are often multiple contacts along the catheter.

In the view of the limitations of the existing works, we propose a new multi-section kinematic model for tendon driven catheters, aiming for both real-time intrinsic force sensing and steering control. The model can accurately predict the 3-dimenional variable curvature along the catheter under large deflection with the consideration of the internal friction, the tension applied on the tendons and the applied external forces. The model allows the external force to be applied at arbitrary location on the catheter; it can also cope with multiple contacts. Meanwhile, the model is computational fast, the update rate of 400 Hz. Therefore this model can be used to control the interaction between the catheter and endocardium in real-time. In this study, we validated the model using a robotic platform which steers a catheter with 4 tendons with tension feedback. The experimental results show that the model can accurately predict the catheter shape under large deflection. Based on the catheter model, we developed an algorithm to estimate the contact force based on the catheter tip tracking and tension feedback. The validation results show that 3-dimensional contact forces can be estimated accurately using the proposed method.

II. Modular Approached Kinematic Model

Most commonly used medical catheters consist of a stiffer catheter shaft and flexible catheter tip, which leads to the assumption that the kinematics of a catheter can be described employing a large deflection model for cantilever beams. The previously mentioned efforts in deriving a catheter's kinematics, its behaviour considering external loading and internal friction is still considered a major challenge in the field. In the context of prior research, we develop a multi-section kinematics model based on Bernoulli-Euler's hypothesis to describe large deflection of a catheter tip, external load on tip end, and friction in the tendon channels. The multi-section kinematics model for the catheter deflection in 3D is solved analytically, and modified to estimate the catheter shape under external load and tension with the aim to estimate the external forces applied to the catheter tip.

A. Tension-based multi-sectional model

A multi-section kinematic model for the catheter has been derived to fit the physical behavior of the helical catheter tip segment as proposed in [12]. It made it possible to achieve flexibility and variable stiffness by compression as show in Fig. 2.

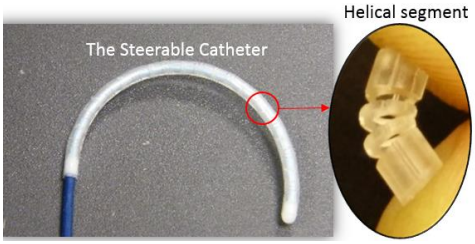

Fig.2. The helically segmented catheter tip and the segment.

Therefore friction inside the tendon channels, deformation of a single element, and variable Young's modulus due to compression were considered in this model.

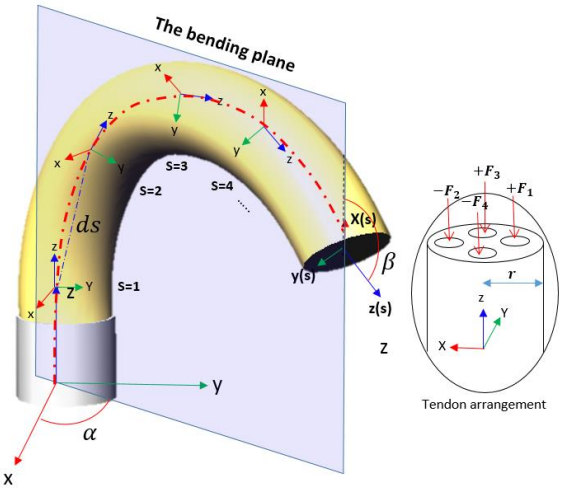

Fig.3. The schematic diagram for the multi-section model

There are four tendons attached to the catheter tip. These tendons are arranged to the four cardinal direction; resulting in a 3-dimensional workspace of the catheter. The coupled two tendons control the direction of catheter tip bending about one axis, thus the tension on x and y axes can be represented as follow:

$$F_{tx} = F_1 - F_2 \qquad F_{ty} = F_3 - F_4 \tag{1}$$

Based on experimental observation of the catheter tip deflection, the bending of the tendon driven catheter tip lies in a single 2-dimensional plane which is referred to as the bending plane in the following. The z-axis rotation angle α_t by tension between the bending plane and x-axis is calculated using the distribution of tendons as Eq. (2)

$$\alpha_t = \tan^{-1}\left(\frac{F_{tx}}{F_{ty}}\right) \tag{2}$$

Bending moment on the bending plane at any section in catheter tip is calculated using magnitude of the tensions as Eq. (3).

Preprint submitted to 2016 IEEE/RSJ International Conference on Intelligent Robots and Systems. Received March 1, 2016.

$$\mathrm{M}_B(s) = r\sqrt{{F_{tx}}^2 + {F_{ty}}^2} \tag{3}$$

Where, r is radius of the catheter tip as shown in fig. 3. Generally, a bending moment between sections is described by the Bernoulli-Euler bending moment and curvature relationship as Eq. (4)

$$\frac{dk}{ds} = \frac{1}{EI}\frac{dM}{ds} \tag{4}$$

k is a curvature at any point of the catheter tip. E is young's modulus, and I is second moment of inertia EI is the flexural rigidity depending on material and geometrical characteristics of the catheter tip. Eq. (4) is re-written using a bending angle and a bending moment relationship ($\theta = \mathrm{ML/EI}$). A bending angle difference between two sections, $d\theta_b(s)$ is obtained after differentiation of θ respect to s as Eq. (5).

$$d\theta_b(s) = \frac{M}{EI}ds \tag{5}$$

where ds is the length between two sections. Using the combination of rotation of the small section length (ds) a geometrical curve can be presented as fig **4**.

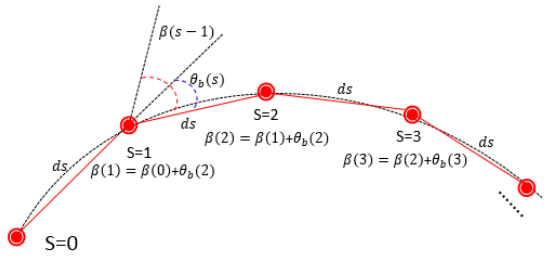

Fig.4. The bending angle assembling at each section

In the multi-section model, a single helix structure was discretized by 4 section, so that the discretized section ds was 1.125mm and total section number was 50 for the entire catheter tip. This number was determined experimentally. Thus, we assume that a position $P_s(x, \mathrm{z})$ at a section on the bending plane is defined using a rotation as Eq.(6-7) as in [13].

$$x(\mathrm{s}) = \sin\beta_t(s)\, ds \tag{6}$$

$$z(\mathrm{s}) = \cos\beta_t(s)\, ds \tag{7}$$

where x is the horizontal position and z is the vertical position. Each position of discretized section on the Cartesian co-ordinate system was presented by a rotation using the bending angle $\beta_t(s)$ with the tension on the bending plane as Eq. (8)

$$\beta_t(s) = \beta_t(s-1) + d\theta_b(s) \tag{8}$$

The bending angle at s node $\beta(s)$ is defined by the previous bending angle at $\beta(s-1)$. Position $P_s(x, z)$ is updated as:

$$P_s(\delta_x, \delta_z) = [\sin\beta_t(s)\, ds \quad cos\beta_t(s) ds] + P_s(s-1) \tag{9}$$

The configuration of the catheter tip on the bending plane is rotated on z-axis using α_t as Eq. (2), thus the 3-dimensional position (P) of multi sections are

$$\mathrm{P(s)} = [\sin\alpha_t(s)\, P_s(x) \quad cos\alpha_t(s) P_s(x) \quad P_s(\mathrm{z})] + \mathrm{P}(s-1) \tag{10}$$

If $\beta(s)$ is purely linear with respect to any section, $d\theta_b(s)$ is of equal value at all nodes. The derived relation is similar to the constant curvature deflection model. However, the bending angles at each individual node have different values due to friction in the tendon channels. In addition, compression and variable Young's modulus due to the helix structure in the used catheter tip have to be considered.

B. Tendon friction

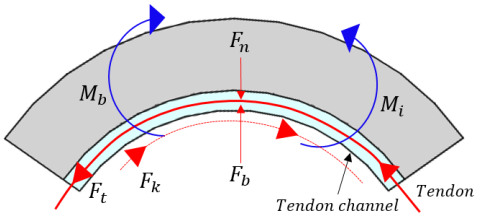

Fig.5. The kinetic friction in the tendon channel

A kinetic friction force (F_k) is primary cause of friction during catheter steering. F_k occurs as normal force F_n on the surface of the tendon channel [9]. The tension F_t is applied along the beam shape, thus tension F_t is mostly distributed as tangent force on the surface. Instead of considering F_t to calculate F_n, we considered the body force F_b as shown in Fig. 5. Elasticity of the catheter tip generates body force F_b when the catheter tip is bent. We assume that F_b acts as normal force F_n between the tendon and the surface ($F_b = F_n$). The internal body moment M_i is defined by $\mathrm{F}_b L(S)$. Where $L(S)$ is the length between first section (n=1) and any point of the catheter tip. Therefore, F_b can be derived using Eq. (5), and F_k can be calculated as Eq.(11).

$$F_k = \frac{\theta EI}{L(s)}\frac{1}{ds}\mu^k + F_k(s-1) \tag{11}$$

Where the kinetic coefficient μ^k is considered as friction between two different materials. The kinetic friction at node (s) involves the kinetic friction at the previous $(\mathrm{s}-1)$. Now, the bending moment $\mathrm{M}_B(s)$ in Eq(5) is re-updated using both kinetic friction forces.

$$\mathrm{M} = (F_t - F_k)\mathrm{r} \tag{12}$$

where F_t is the tension.

C. Helix compression

When tension is applied to the catheter tip, all of the discretized section are simultaneously bent and compressed. If the catheter tip is deflected by only applying tension, the

direction of the compression follows the neutral axis of the discretized section at a section of the catheter tip. The position of each element can be rewritten considering shear. Thus, Eq. (9) involves shear deformation as Eq. (13).

$$P_s(\delta_x, \delta_z) = [\sin\beta_t(s)\left(ds - \frac{F_t ds}{GA}\right), \cos\beta_t(s)\left(ds - \frac{F_t ds}{GA}\right)] \quad (13)$$

where G is shear modulus ($2 \times 10^6 N/m^2$), A is area on which the force acts, and F is a tension including the friction forces. The stiffness of the helix is varied by the compression of the helix structure, for which E has been obtained experimentally. Based on experimental observation, the Young's modulus was varied by tension as Eq. (14).

$$\mathrm{E} = \mathrm{E}_i e^{\frac{F_t ds}{GA}} \quad (14)$$

Where E_i is initial young's modulus. In this studying, the E_i was given $5.1 \times 10^6 N/m^2$. The difference bending angle between two section, $d\theta_b(s)$ in Eq.(5) is updated using Eq. (14)

D. External Load

During the catheter ablation, the catheter tip is deflected by interaction with heart. In particular when the catheter tip is carried into the left atrium through the septum to ablate target tissue, the catheter tip shape deformation based on external force has to be considered. Therefore, an external load on catheter tip was studied as a point load at any point on the catheter tip; it was gradually achieved using the multi section model. We can assume that applied the external load is known. Also, the external load ($F_e = [F_x\ F_y\ F_z]$) acts from first element (n=1) to the external force contact position on the catheter tip. Deformation P_d by F_e is calculated as Eq. (15).

$$P_d = F_e \frac{L(s)}{GA} \quad (15)$$

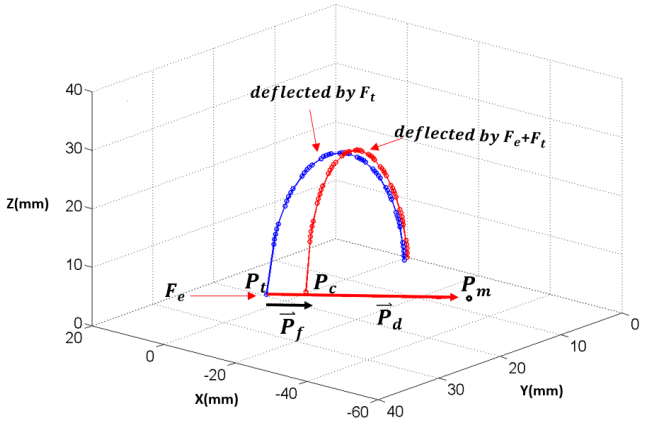

Fig.6. The external load simulation result

The position of each section, P_s is relocated by the deformation P_d, and also young's modulus (E) is recalculated using P_d, Eq. (14) is rewritten as follow:

$$\mathrm{E} = \mathrm{E}_i e^{GF_t\frac{ds}{GA} + F_e\frac{L(s)}{GA}} \quad (16)$$

As shown in Fig 6, the catheter tip shape is decided by a combination of tension and external load. In this model, the shapes generated by tension and external load are separated; the external load is applied to the already estimated catheter shape by tension. Thus, the bending moment at each section is recalculated by cross product of distance $(P_e - P_n)$ and external force F_e as $\mathrm{M}_e(\mathrm{s}) = (P_e - P_n) \times F_c$ as shown in Fig.6. Where P_e is contact location, P_n section position, and F_c is contact force. Furthermore, we assume that the bending of each section lies in a 2-dimensional plane. Therefore, the bending moment in the bending plane of each section is calculated as

$$M_e = \frac{F_z}{|F_z|}\sqrt{M_e(x)^2 + M_e(y)^2} \quad (17)$$

with the contact force along the z-axis F_z used to define direction of M_e. The bending angle of each element is calculated using the Young's moduli from Eq.(16). M_z at each section is calculated independently using torsional stiffness GJ instead of EI. Therefore, the z-axis rotation angle, $\alpha(\mathrm{s})$ is obtained as the Eq (2). The bending angles $\beta_e(s)$ and $\alpha_e(\mathrm{s})$ resulting from external load are summed with the $\beta_t(s)$ and $\alpha_t(s)$ by tension as Eq. (18-19).

$$\alpha(\mathrm{s}) = \alpha_t(s) + \alpha_e(s) \quad (18)$$

$$\beta(\mathrm{s}) = \beta_t(s) + \beta_e(s) \quad (19)$$

The resulting angles and deformations are applied to Eq. (10) to reshape the catheter tip in the bending plane.

$$P_s(\delta_x, \delta_z) = \left[\sin\beta(\mathrm{s})\left(ds - \frac{F_t ds}{GA}\right), \cos\beta(\mathrm{s})\left(ds - \frac{F_t ds}{GA}\right)\right] + P_d(s) + P_{s-1}(x, z) \quad (20)$$

To be represented in 3D

$$\mathrm{P(s)} = [\sin\alpha(\mathrm{s})\,P_s(x),\ \ cos\,\alpha(\mathrm{s})P_s(x),\ \ P_s(\mathrm{z})] + \mathrm{P}(s-1) \quad (21)$$

E. Contact Force Estimation

The estimated shape variation of the catheter by external load can be used to determine the contact force on the catheter tip end employing position sensing instead of shape reconstruction. Key principle of the contact force estimation based on position sensing is that the catheter tip position P_t by tension and measured catheter tip position P_m have difference as P_d, when the catheter tip generates contact force on target tissue. The P_d is generated by the contact force F_c, and is proportioned to F_c. As a first step of this force estimation the catheter shape based on the applied tensions P_t has to be determined, and then the direction of contact

force ($\vec{F}_c$) is defined using the position difference ($\vec{P}_d = P_m - P_t$) as Eq.(22) as shown in Fig. 6.

$$\vec{F}_c = \vec{P}_d \tag{22}$$

Applying $\vec{F}_c$ to the configured catheter shape causes larger displacement in the catheter tip position. Thus, the unit vector of the direction of the contact force, ($\hat{F}_c$) is scaled down by $u(< 0.01)$ and applied to calculate the bending moment $M_c(s)$ by contact force at each section. New catheter position P_c is obtained by applying $M_c(s)$ to the catheter shape configuration based on tension, and then a motion vector ($\vec{P}_f$=$P_c - P_t$) is calculated. Using the proportion assumption, F_c is estimated using scale between $\vec{P}_f$ and $\vec{F}_c$ as Eq. (23).

$$F_c = \hat{F}_c u \frac{\vec{P}_d}{\vec{P}_f} \tag{23}$$

III. MODEL VALIDATION

The introduced multi-section model for the catheter tip were validated through two different experiments. First experiment was designed to examine the catheter shape estimation using the multi-section model. Second experiment was implemented to validate the contact force estimation and the external load model. Contact force is estimated through the catheter tip shape estimation by external load, thus the external load model was examined through the force estimation experiment.

In both of the experiment, the miniaturized linearly-actuated tendon driven platform was used to apply tension, and to take the introduced advantages of the linearly-actuated tendon driven such as backlash prevention, less slack and tangled tendon [14]. Also the tension was measured using the cantilever beam structured tension sensor during catheter steering as shown in Fig. 7.

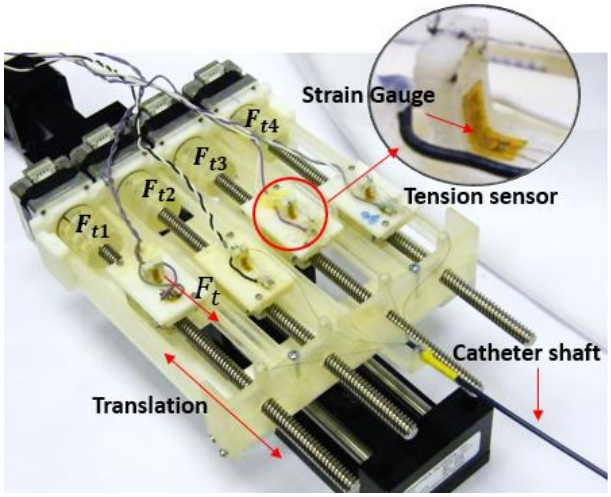

Fig. 7. Miniaturized linearly actuated tendon driven platform

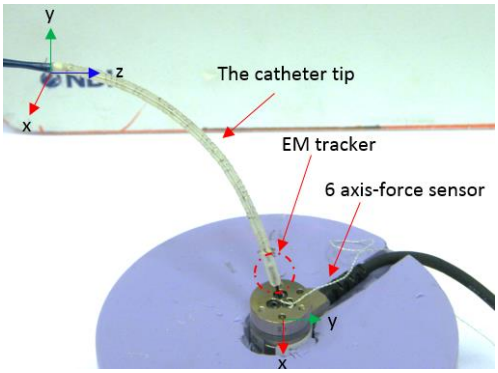

Fig.8. The force estimation experiment set-up

A. Catheter shape estimation by tension

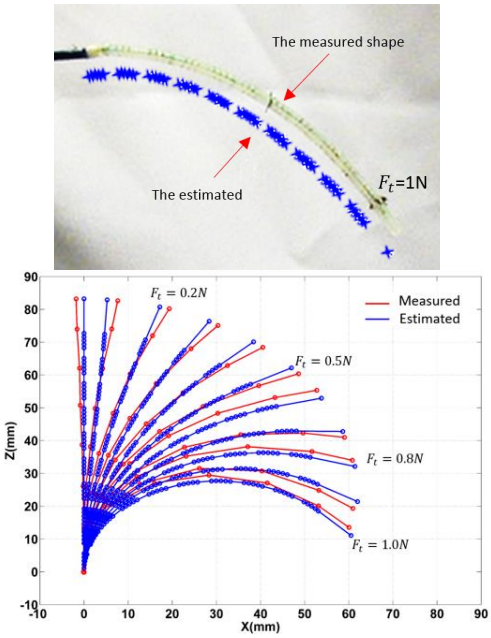

Fig.9 the estimated catheter tip deflections ($\boldsymbol{F_t = 0 \sim 1N}$)

The tension was given 0N to 1N, and the catheter shape was measured using a RGB camera. The measured catheter tip shapes as shown in Fig. 9. It showed that the sections closer to the end has less deflection. This physical behavior was derived using the kinetic friction and the variable young's modulus model. Thus, the estimated catheter tip shape is well matched with the measured catheter tip shape. During this experiment, the average of the end position error was about $\pm$ 2.5 mm, and the maximum position error was about 3.5 mm when $F_t = 0.4N$.

B. Contact force estimation

During the force estimation, the catheter shaft was clamped as fixed end condition, and the catheter tip position was provided using a magnetic position tracker (NDI Aurora tracker). The catheter tip was steered using the linearly-actuated catheter steering platform to generate contact force on the 6-axis force sensor. The benchmark force values were re-oriented and matched with estimated contact force. The results are as

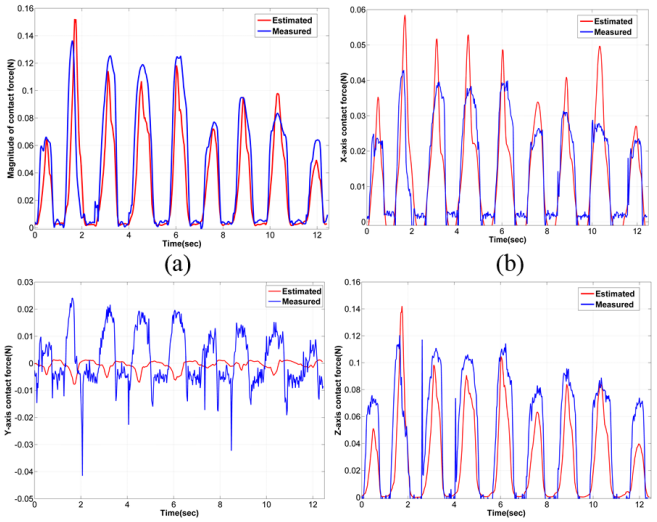

Figure 10 The contact force estimation results: (a) magnitude, (b) x-axis, (c) y-axis, and (d) z-axis

During the contact force estimation, the negative direction of F_{tx} was major tension value, and it was increased and decreased repeatedly from 0N to over 2N. The F_{ty} was maintained about 0.1N. Magnitude errors of the estimated contact forces on individual axis, x y, and z are 0.0012N, 0.0022N, and 0.0162N respectively. This leads that the magnitude of the contact force has accuracy about 0.0117N. The contact forces were estimated in real time, the calculation frequency is 350Hz except sensor data transfer.

IV. Discussion

The multi-section model for the catheter tip was validated through the experiments of the shape estimation and the contact force estimation. These experiments obtain satisfactory accuracies. Moreover, the both estimation were run in real time, the update rate is 400Hz. However, if the tension is released after high tension is over 3N, the catheter tip shape has larger hysteresis. It was a major reason of the catheter shape estimation error. Number of the section in the model is an undefined variable, and the deflection of catheter tip can be changed depending on the number. Thus, it is required defining the section number experimentally, or additional optimization will be needed. Another consideration is in the contact force estimation. During the experiment, the tension applied steadily. If the tension is varied dynamically, the force estimation has to consider dynamic model. However, during the catheter ablation procedure, the catheter can be steered with almost steady velocity, and less acceleration for safety. Thus, the analytical solution of the contact force estimation has a possibility to be applicable for the catheter ablation.

V. Future work & Conclusion

The multi-section model for catheter tips were derived, and introduce in this paper. The model can accurately predict 3-dimenional the catheter deflection with the consideration of internal friction, the tension applied on the tendons and applied external forces. Moreover, the real-time intrinsic force sensing and the catheter shape estimation are achieved using the proposed new-multi-section kinematic model for tendon driven catheters. During the model validation, the model showed satisfactory results such as 2.5mm position error and 0.0117N contact force error. However, the required improvements such as optimization of the multi-section number, consideration on hysteresis of catheter tip deflection and consideration about dynamic case were discussed. Nonetheless, the catheter tip deflection analysis using the multi-section model is still applicable to catheter tip control, and to estimate contact force. Moreover, the discretization of the catheter tip in model makes possibly achieve multi contact forces estimation on any points on the catheter tip and the multi contacted shape estimation for interaction control.

Reference

[1] Di Biase, L., et al, Relationship between catheter forces, lesion characteristics, “popping,” and char formation: experience with robotic navigation system. Journal of cardiovascular electrophysiology, 20(4), pp.436-440. 2009

[2] Thiagalingam, A. et al, Importance of Catheter Contact Force during Irrigated Radiofrequency Ablation: Evaluation in a Porcine Ex Vivo Model Using a Force-Sensing Catheter. Journal of cardiovascular electrophysiology, 21(7), pp.806-811, 2010.

[3] K. Xu and N. Simaan, “An investigation of the intrinsic force sensing capabilities of continuum robots,” IEEE Transactions on Robotics, vol. 24, no. 3, pp. 576–587, 2008.

[4] Camarillo DB, Milne CF, Carlson CR, Zinn MR, Salisbury JK. Mechanics modeling of tendon-driven continuum manipulators. Robotics, IEEE Transactions on. 2008 Dec;24(6):1262-73.

[5] Y. Ganji and F. Janabi-Sharifi, “Catheter kinematics for intracardiac navigation,” IEEE Trans. Biomed. Eng., vol. 56, no. 3, pp. 621–632, Mar. 2009.

[6] Rucker DC, Webster III RJ. Deflection-based force sensing for continuum robots: A probabilistic approach, IEEE/RSJ International Conference on In Intelligent Robots and Systems (IROS), 2011 Sep 25 pp. 3764-3769.

[7] Khoshnam M, Skanes AC, Patel RV. Modeling and estimation of tip contact force for steerable ablation catheters. Biomedical Engineering, IEEE Transactions on. 2015 May;62(5):1404-15.

[8] J Back, T Manwell, R Karim, K Rhode, K Althoefer, H Liu, Catheter Contact Force Estimation from Shape Detection using a Real-Time Cosserat Rod Model, IEEE/RSJ International Conference on Intelligent Robots and Systems (IROS), pp 2037-2042, 2015

[9] Jung J, Penning RS, Ferrier NJ, Zinn MR. A modeling approach for continuum robotic manipulators: effects of nonlinear internal device friction. InIntelligent Robots and Systems (IROS), 2011 IEEE/RSJ International Conference on 2011 Sep 25 (pp. 5139-5146). IEEE.

[10] Tunay, I. “Spatial Continuum Models of Rods Undergoing Large Deformation and Inflation”. IEEE Transactions on Robotics, 29(2), p. 297-307. 2013

[11] M. A. Crisfield. Non-linear Finite Element Analysis of Solids and Structures – Vol 1. John Wiley & Sons Ltd., Chichester, England, 1991.

[12] A. Ataollahi, R. Karim, A. Soleiman Fallah, K. Rhode, R. Razavi, L. Seneviratne, T. Schaeffter, and K. Althoefer. "3-DOF MR-Compatible Multi-Segment Cardiac Catheter Steering Mechanism. IEEE Transactions on Biomedical Engineering, 2013 (preprint online)

[13] Tarsicio Belendez, Critian Neipp and Augusto Belendez, Numerical and Experimental Analysis of a Cantilever Beam: a Laboratory Project to Introduce Geometric Nonlinearity in Mechanics of Materials, International Journal Engineering Education, Vol. 19, No. 6, pp. 885-892, 2003

[14] J. Back, R. Karim, Y. Noh, K. Rohde, K. Althoefer, and H. Liu, Tension Sensing for Linear Actuated Catheter Robot, International Conference of Intelligent Robotics and Application, Vol. 9245, pp. 472-482, Aug, 2015